Particle growth in a sputtering discharge

D. Samsonov and J. Goree[a)]
Department of Physics and Astronomy, The University of Iowa, Iowa City, Iowa 52242

(Received 22 October 1998; accepted 7 May 1999)

Submicron to micron size particles are produced in the gas phase of sputtering discharges. These particles can contaminate thin films grown by sputter deposition. On the other hand, particle production in a discharge can be desirable when used for manufacturing fine powders. Here, experimental results are presented demonstrating particle production in an argon discharge, using a variety of target materials. The rate of particle growth varied widely, depending on the target material. Particles grown to 300 nm–5 μm, usually have one of two different shapes. Compact particles with a nearly spherical shape were produced by sputtering graphite, titanium, tungsten, and stainless steel targets, while filamentary-shaped fractal particles formed when sputtering aluminum and copper targets. Particle growth was also observed for a target made of an insulating material. © *1999 American Vacuum Society*. [S0734-2101(99)05605-5]

I. INTRODUCTION

Particulate contamination of thin films is a concern in many industries, including semiconductor manufacturing. Particulates[1] are formed either in the gas phase of the plasma or by flaking off deposited films from wall surfaces. They then become negatively charged and electrostatically trapped in a plasma, where they can increase in size.[2] When the plasma is turned off, or even sooner than that, they can fall onto or be transported otherwise to the substrate. With 0.18 μm feature sizes on a semiconductor wafer, a particle of diameter of 90 nm may result in a killer defect. Particles of this size, and some much larger, are known to grow in plasma processing discharges, including sputtering sources.

In sputtering plasmas, particle contaminates grown in the gas phase have been reported for several kinds of sputtering targets and plasma sources. Selwyn *et al.* reported particle growth in a SiO_2 sputter deposition plasma.[3] The most significant mechanism of particulate production in such a plasma is the condensation of sputtered target material in the gas phase. Jellum *et al.* observed growth of aluminum particles[4] as well as carbon and copper particles[5] using both dc and rf sputtering. Carbon particle production in an argon rf sputtering discharge was also observed by Praburam and Goree.[6] Growth of carbon particles in 15 kHz helium plasma was extensively studied by Ganguly *et al.*, by Garscadden *et al.*, and by Haaland *et al.*.[7–9]

In addition to sputtering discharges, other types of plasma processing plasmas produce particles too. Chemical vapor deposition (CVD) plasmas are prone to particle formation, as has been reported by many authors, including those of Refs. 10–23. Particles can grow either by homogeneous nucleation, as in argon-silane discharges,[11] or by heterogeneous processes. The latter includes cluster formation on an electrode surface, which leads to subsequent particle growth in the surrounding plasma in the case of a SiH_4/NH_3 discharge.[13] Etching plasmas produce particles grown in the plasma itself and by deposited films flaking from wall surfaces.[2,24–27]

On the other hand, particle production in a plasma can be a desirable way of manufacturing nanoparticles of various materials. Synthesis of silicon nitride particles for ceramics was demonstrated by Buss and Babu[28] using a pulsed rf discharge. Magnetron sputtering was used by Hahn and Averback[29] to produce nanoscale particles of pure metals, binary alloys, intermetallics, and ceramics, which was not possible by conventional thermal evaporation. Chow *et al.* demonstrated[30] synthesis of nanocomposite materials by utilizing sputtering dc discharge. They produced a so-called phase-separated material consisting of molybdenum nanoparticles embedded in an aluminum matrix. The latter may have applications in high temperature coatings and nanoscale dispersion-strengthened coatings.

In this article we report phenomenological observations of submicron to micron particles formed in the gas phase of a sputtering discharge for a variety of target materials. Particles that fell to the lower electrode were examined by scanning electron microscopy (SEM) after the plasma was extinguished. We found that the growth rate varies widely according to the target material, and that particles grow in either a compact shape that is nearly spherical or with a filamentary-shaped fractal morphology. The plasma used here was a capacitively-coupled rf discharge, although the particle growth mechanisms are likely to be similar in other types of discharges as well.

II. METHOD

A rf capacitively coupled discharge was formed between two parallel-plate water cooled electrodes, shown in Fig. 1. In this device, which is similar to the one used previously by Praburam and Goree,[31] the electrodes were 8 cm in diameter and were separated by 2 cm. The lower electrode, which was grounded, was made of stainless steel, and it was not sputtered. The powered upper electrode was covered with the sputtering target, which was clamped in place by a stainless ring [Fig. 2(c) of Ref. 31]. Target erosion after many hours

a)Author to whom correspondence should be addressed; electronic mail:

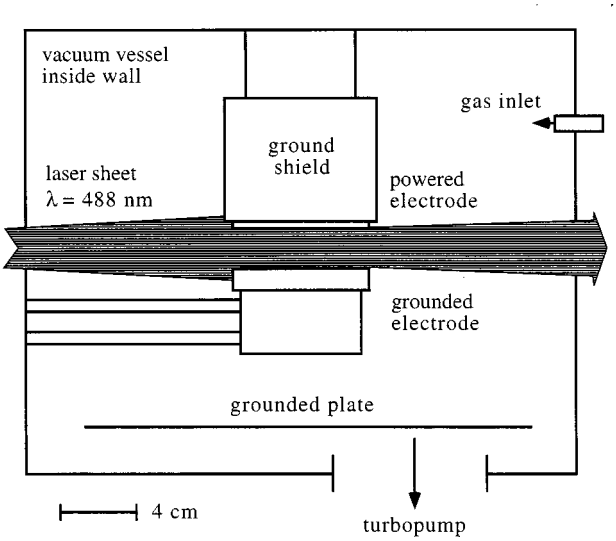

FIG. 1. Sketch of the experimental setup, side view. A vertical sheet of argon laser light illuminates the particulates.

of exposure to a plasma was observed only in the central part (4–4.5 cm diam) of the powered electrode. The generator was coupled to the lower electrode through an impedance matching network and a coupling capacitor. A power of 100 W (forward minus reverse) was applied, developing a dc self-bias of −300 V. Argon pressure was maintained at 400 mTorr. The gas flow was 60 sccm for most of the experiments.

Sputtering targets installed on the powered electrode were made from different materials, including graphite, copper, titanium, stainless steel, tungsten, and aluminum. As a test, one target was coated with ''Torr Seal'' vacuum epoxy.

The diagnostics used in the experiment included discharge glow imaging, laser light scattering and optical extinction to detect the particles *in situ* in the plasma, and *ex situ* SEM of the particles.

Using LLS we detected particles as they formed in the gas phase. A sheet of laser light was formed by passing an argon-ion laser beam through a cylindrical telescope to illuminate a vertical plane in the vacuum vessel. A video camera that viewed this plane was equipped with an interference filter to select the laser wavelength (488 nm). This method of particulate detection was used previously by many experimenters, including Selwyn *et al.*,[24] Hareland *et al.*,[32] and Praburam and Goree.[33] The video was recorded on a VCR and then digitized with a frame grabber.

To measure the growth of the particle size, we interrupted the discharge at different times in a repeated series of experiments. Some of the particles fell onto a thin stainless steel foil substrate placed on the lower electrode. We then placed the substrate, with the particles intact, in a Hitachi S-4000 field emission scanning electron microscope. Surface melting by the electron beam was avoided by minimizing the specimen's exposure to the beam. The particle diameters were measured directly on the micrographs by a caliper. Fifteen measurements were taken per micrograph and then the average and standard deviations were calculated. For nonspherical shapes, both the longest and shortest distances across a given particle were measured. Error bars were computed as the root mean square (rms) of all the measurements from a micrograph, including both measurements for the nonspherical particles. In the case of particles grown from sputtering graphite, the uncertainties in the size measurement are attributable to diffuse particle boundaries.

The particle number density was measured *in situ* by laser light extinction. The intensity of a laser beam directed through the chamber was compared with and without particles to determine the extinction. Using Mie scattering theory, along with the refractive index parameters listed in Ref. 34, this yielded the particle number density. The particle size measured by SEM was used as an input parameter in this calculation.

III. RESULTS

Particle growth in the gas phase was observed for all the sputtering targets we tested. Our tests with graphite sputtering targets indicated that particle formation required a low vacuum base pressure of $<10^{-6}$ Torr, suggesting that the presence of nitrogen or other gas impurities can inhibit particle formation. Particles were found to grow regardless of the presence of a gas flow.

There were so many particles present in the plasma that they formed what appeared to be an aerosol cloud when illuminated by laser light. This cloud filled the entire interelectrode space. Particles presumably formed in the interelectrode region, and many of them flowed outward. The particle cloud developed as follows.

When the discharge was first switched on, it was free from particles. After a few seconds or minutes, depending on the target material (see Table I), the particulate cloud was detected by the video camera. The particle size grew over time, thereby scattering more light and making the cloud appear to become thicker. A LLS image, Fig. 2, shows that the particle cloud filled the entire volume between the electrodes, except for the thin sheaths near the electrodes. It was densest close to the powered (upper) electrode. We found that the cloud was not limited to the interelectrode region, but that it spread radially far beyond the electrodes, apparently due to outward particle flow from the interelectrode region. After the particle size grew to a critical diameter of 120 nm, the discharge became unstable. It exhibited two instability modes, the ''filamentary'' and the ''great void'' modes, which are described in detail in Ref. 34. Toward the end of the instability cycle there was an empty region, or void, in the particle cloud. The void expanded as the particles grew in diameter until it filled nearly the whole interelectrode region. This marked the end of a growth cycle. When a new cycle began, fresh particles began growing in the void. The duration of this cycle varied with target material, as listed in Table I. To compare SEM images of the particles, we always interrupted the discharge at the end of the first instability cycle, before any new particles appeared. In this way, we were able to image only the first generation of particles.

TABLE I. Timing of particulate growth with electrode targets made of various materials. Times are indicated in h, min, and s after the discharge was ignited. The sputtering yields are based on Ref. 37. The particle diameters were measured *ex situ* by electron microscopy at the end of the growth cycle. Note that the particle size at the end of the cycle is the same for all the nonfractal particles, regardless of the growth rate. The size distribution is indicated by the ± in the right-hand column. Epoxy sputtering produced a measurable particulate cloud, but we were unable to image its particles afterwards using SEM. (Torr seal is manufactured by Varian.)

Electrode material	Time of detection of particles	Duration of the growth cycle	Sputtering yield (at 300 eV)	Particle size (nm)
Copper	15 s	5 min	1.59	Fractal 5500±3500
Torr Seal epoxy	20 s	3 min	N/A	N/A
Graphite	30 s	4 min 20 s	0.1[a]	343±11
Titanium	2 min	3 h	0.33	360±65
Stainless steel	5 min	1 h 24 min	0.76 (for Fe)	350±70
Tungsten	7 min	2 h	0.4	360±50
Aluminum	10 min	50 min	0.65	Fractal 1500±700

[a]At 400 eV.

The time series for the particle size and number density are shown in Fig. 3. Initially, the particle size increased rapidly, and then it slowed down. The particle density developed, however, with an opposite trend, a high initial value that declined as the particle size grew.

This temporal development is similar to the growth of particles in a silane discharge, as shown, for example, in Fig. 4 of Boufendi and Bouchoule.[10] The only significant difference between the silane and the sputtering discharges is the growth rate, which is much faster for silane. This similarity suggests that similar growth mechanisms may be at work. For silane, Boufendi and Bouchoule[10] proposed that particles grow in three stages. In the first stage crystallites form by nucleation of atomic or molecular species. Due to their small size, we were unable to detect this first stage in our experiment. In the second stage, these crystallites grow by colliding into one another and sticking, a process that is often called coagulation or agglomeration. This causes rapid growth in the particle size and a commensurate decrease in the particle number density. This is possible because small particles have smaller electric charges and significant charge fluctuations,[1] so that the Coulomb repulsion between the negatively charged particles is not severe. In the third stage, particles have enough negative charge to suppress coagulation, and they can grow only by the slower process of accretion, i.e., collecting ions and/or neutral species from the gas phase. In this third stage, the growth rate is smaller than in the second, and the number density is approximately constant.

If we now consider now the desirable application of these growth processes for synthesizing nanoparticles, it is necessary to quantify the production rate. Since the growth occurs under vacuum conditions, the production rate will never be extremely high, although it may still be useful for certain high-value-added applications that require nanoparticles that cannot be synthesized in other ways. The production rate can be computed as follows. The total mass of a particulate cloud is $M=(4/3)\pi r^3 \rho n_d V$, where r and ρ are the particle's radius and mass density, respectively, n_d is the particle number density, and V is the volume occupied by the cloud. The production rate is found by dividing M by the growth cycle period. For a graphite target, the production rate is approximately 0.2 mg/min. The corresponding rate in a silane/ammonia discharge is a much faster, 1.67 mg/min, as re-

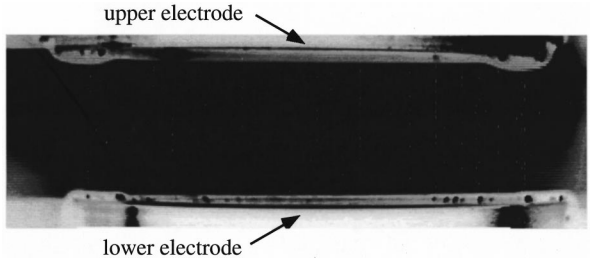

FIG. 2. Image of LLS from the particulate cloud, side view. A vertical laser sheet illuminated the interelectrode space. Darker gray corresponds to higher particle number density. The particles are mostly trapped between the electrodes. The cloud extends farther beyond the electrodes in the horizontal direction than is shown here.

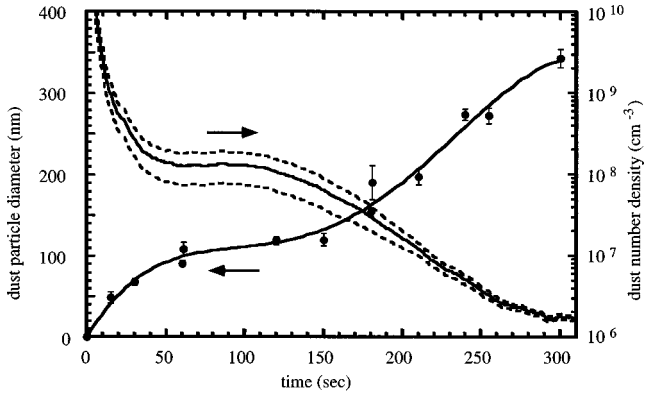

FIG. 3. Particle number density and size for the graphite target vs time. The particle size was measured *ex situ* by SEM in a repeatable series of experiments interrupted at different times. To determine the particle number density we measured the extinction of laser light passing through the particulate cloud, which was then converted into the number density using Mie scattering theory. The dashed curves for number density indicate the error bars in this measurement. (Reprinted with permission from Ref. 34).

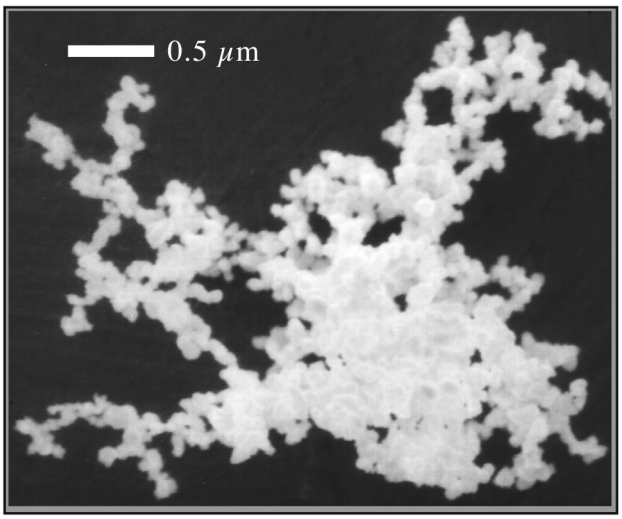

FIG. 4. Electron micrograph of particles grown from sputtering a copper target. The particles have a filamentary fractal shape. As with all micrographs, these show particles grown for one full growth cycle. The duration of a growth cycle varies with the target material; see Table I.

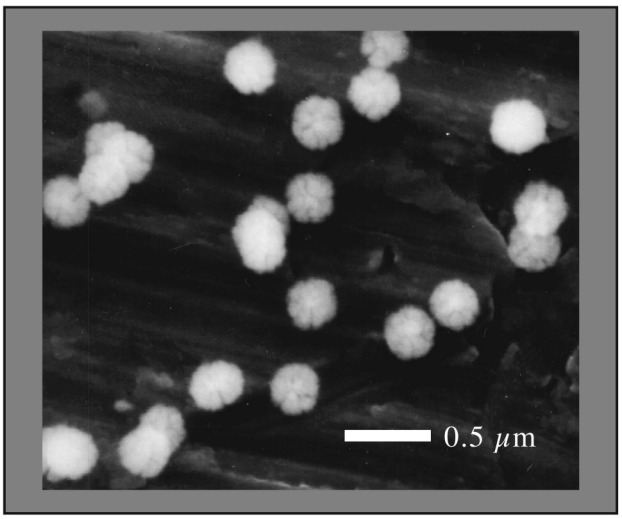

FIG. 6. Electron micrograph of particles grown from sputtering a carbon target. The particles have a bumpy spherical shape. (Reprinted from Ref. 34).

ported by Anderson *et al.*.[13] Particle growth rates are always higher in reactive gas discharges than in a sputtering discharges because of the higher densities of reactive species. However the sputtering discharge has an advantage that it can produce particles from almost any solid material that can be sputtered without decomposition. In our experiment the particles fell to the bottom wall of the chamber after the discharge was turned off. As a manufacturing tool it would be necessary to redesign our apparatus to provide a more effective method of collecting particles.

Different materials exhibited the same particulate growth and instability pattern, but the timing was different (see Table I). The growth cycle for the aluminum target had a long delay before the particles were detected. This is probably due to the oxide layer on the surface of aluminum, which had to be sputtered off before the sputtering of aluminum started.

Particles grown from different materials had different shapes. Some particles were filamentary fractals, like those grown from copper and aluminum (Figs. 4 and 5). In contrast carbon particles (Fig. 6) had a bumpy spherical shape. Other materials formed compact coagulants of a few spheres, like titanium (Fig. 7) and stainless steel (Fig. 8). Tungsten formed compact agglomerates (Fig. 9).

IV. DISCUSSION

Most commonly it is assumed that particle growth in a plasma occurs in several steps. At an early stage particles

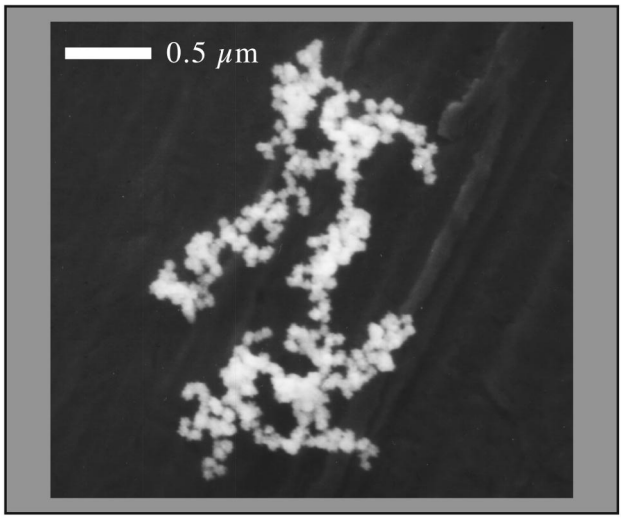

FIG. 5. Electron micrograph of particles grown from sputtering an aluminum target. The particles have a filamentary fractal shape.

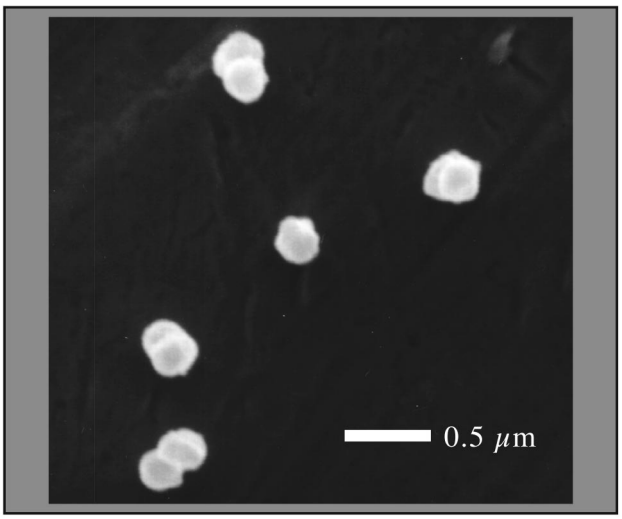

FIG. 7. Electron micrograph of particles grown from sputtering a titanium target. The particles consist of spherical-shaped primary particles that have coagulated into aggregates consisting of a few spheres. The surface of the particles appears smoother than that of the graphite.

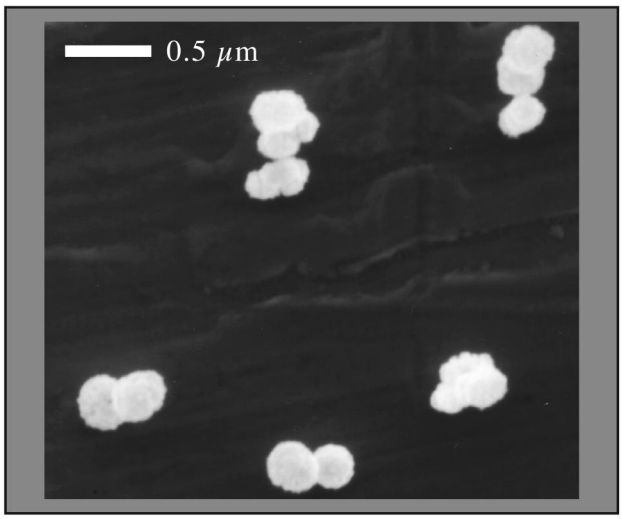

FIG. 8. Electron micrograph of particles grown from stainless steel. The particles appear to be similar to those grown from titanium.

begin as clusters, which can originate either from surfaces[13] or in the gas phase.[10] Then the clusters coagulate, forming the primary particles, and finally, the primary particles agglomerate, forming particles which can be either spongy and filamentary, or compact and spheroidal.

The factor that determines whether the final particle will be filamentary or compact has been suggested by several authors, including Huang and Kushner,[35] to be Coulomb repulsion. All the particles in a plasma are negatively charged (since they would otherwise be expelled from the plasma by the ambipolar electric fields). When the particles have a small charge and a high velocity, they can easily overcome Coulomb repulsion. This leads to the formation of compact or spheroidal agglomerants. On the other hand, when the repulsion is stronger, an incoming particle is more likely to strike the end of a chain of particles than the middle, and this process tends to perpetuate a filamentary or fractal shape.

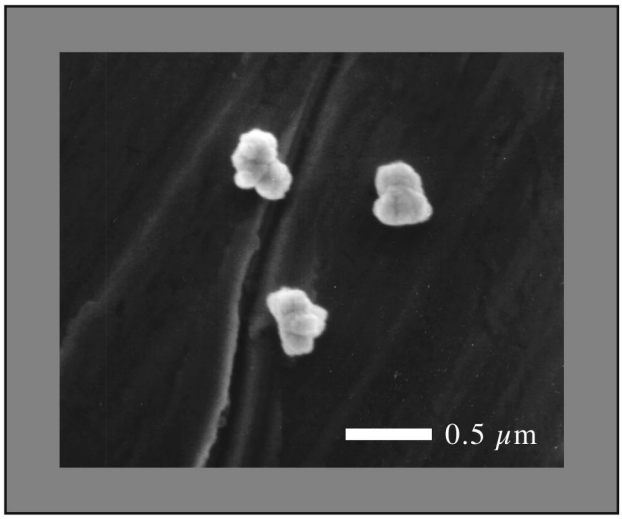

FIG. 9. Electron micrograph of particles grown from tungsten. The particles appear to be similar to those grown from titanium.

The reason the particle is more likely to strike the end of an agglomerate than its middle is that the shielding of the plasma reduces the repulsion produced by more distant elements of the agglomerate. Hence slow moving particles form filamentary fractal agglomerates. This hypothesis was verified by the particle simulation of Huang and Kushner.[35]

In our experiment, most target materials resulted in the formation of either filamentary fractals or compact spheroidal shapes. Fractals were produced from copper (Fig. 4) and aluminum (Fig. 5). Compact particles were formed by sputtering titanium (Fig. 7), stainless steel (Fig. 8), and tungsten (Fig. 9). Based on the model described above, we assume that primary particles made of copper and aluminum tend to have higher velocities than the other particles.

Coagulation is generally the fastest growth process when it is allowed. However, when Coulomb repulsion prevents coagulation, particles can grow only by accretion, i.e., a collection of neutral or ionic species of atoms and molecules. This growth process leads to the growth of spherical particles, according to Haaland *et al.*.[9] These particles tend to have a highly uniform size, and a spherical shape that suggests that late-stage coagulation has not occurred. Spheres meeting this description have been observed in several kinds of plasmas. In Ar/CCl_2F_2 plasmas used for Si etching, Selwyn *et al.*[24] detected spherical particles of a highly uniform size and shape. They had a crystal-like structure and were grown from very small nucleation sites. In our experiment, particles grown by the sputtering of graphite (Fig. 6) have this sort of shape. The surface texture of these spherical particles can be bumpy, giving the particle an appearance that has been described as cauliflower-like.[6] The origin of this bumpy shape has been attributed to either columnar growth during an accretion process[7,36] or to geometric factors, termed fractal recursion, during particle growth.[8]

V. CONCLUSION

Sputtering discharges can generate particles in the gas phase for many materials. Before our experiments, it was known that sputtering of carbon, copper, and aluminum can result in gas phase particle production in a sputtering rf discharge. We have demonstrated here that particle growth also occurs for sputtering of copper, titanium, stainless steel, tungsten, and even Torr Seal vacuum epoxy. In fact, every target material we tested resulted in particle growth when it was sputtered with a capacitively coupled rf argon plasma. The particle size grows over time at a rate that depends on the sputtering yield. Many materials tend to produce particles which are nearly spherical or compact aggregates, while others (like copper and aluminum) produce filamentary fractal-like particles. Particles are confined in the plasma and fall when the discharge is extinguished.

ACKNOWLEDGMENTS

This work was supported by NASA and by the National Science Foundation. The authors thank G. Morfill for providing facilities at the Max Planck Institut für extraterrestrische Physik.

[1]J. Goree, Plasma Sources Sci. Technol. **3**, 400 (1994).
[2]G. Selwyn, J. Heidenreich, and K. Haller, J. Vac. Sci. Technol. A **9**, 2817 (1991).
[3]G. Selwyn, J. McKillop, K. Haller, and J. Wu, J. Vac. Sci. Technol. A **8**, 1726 (1990).
[4]G. Jellum and D. Graves, J. Appl. Phys. **67**, 6490 (1990).
[5]G. Jellum, J. Daugherty, and D. Graves, J. Appl. Phys. **69**, 6923 (1991).
[6]G. Praburam and J. Goree, Astrophys. J. **441**, 830 (1995).
[7]B. Ganguly, A. Garscadden, J. Williams, and P. Haaland, J. Vac. Sci. Technol. A **11**, 1119 (1993).
[8]A. Garscadden, B. Ganguly, P. Haaland, and J. Williams, Plasma Sources Sci. Technol. **3**, 239 (1994).
[9]P. Haaland, A. Garscadden, B. Ganguly, S. Ibrani, and J. Williams, Plasma Sources Sci. Technol. **3**, 381 (1994).
[10]L. Boufendi and A. Bouchoule, Plasma Sources Sci. Technol. **3**, 262 (1994).
[11]L. Boufendi, J. Hermann, A. Bouchoule, B. Dubreuil, E. Stoffels, W. W. Stoffels, and M. L. de Giorgi, J. Appl. Phys. **76**, 148 (1994).
[12]K. Spears, T. Robinson, and R. Roth, IEEE Trans. Plasma Sci. **PS-14**, 179 (1986).
[13]H. Anderson, R. Jairath, and J. Mock, J. Appl. Phys. **67**, 3999 (1990).
[14]P. Haaland, S. Ibrani, and H. Jiang, Appl. Phys. Lett. **64**, 1629 (1994).
[15]J. Perrin, C. Böhm, R. Etemadi, and A. Lloret, Plasma Sources Sci. Technol. **3**, 252 (1994).
[16]C. Hollenstein, W. Schwarzenbach, A. A. Howling, C. Courteille, J. L. Dorier, and L. Sansonnens, J. Vac. Sci. Technol. A **14**, 535 (1996).
[17]C. Hollenstein, J. L. Dorier, J. Dutta, L. Sansonnens, and A. A. Howling, Plasma Sources Sci. Technol. **3**, 278 (1994).
[18]Y. Watanabe and M. Shiratani, Jpn. J. Appl. Phys., Part 1 **32**, 3074 (1993).
[19]Y. Watanabe and M. Shiratani, Plasma Sources Sci. Technol. **3**, 286 (1994).
[20]E. Bertran, J. Costa, G. Sardin, J. Campmany, J. L. Andujar, and A. Canillas, Plasma Sources Sci. Technol. **3**, 348 (1994).
[21]W. Böhme, W. E. Köhler, M. Römheld, S. Veprek and R. J. Seeböck, IEEE Trans. Plasma Sci. **22**, 110 (1994).
[22]R. Seeböck, W. Böhme, W. E. Köhler, M. Römheld, and S. Veprek, Plasma Sources Sci. Technol. **3**, 359 (1994).
[23]W. R. Reents, Jr. and M. Mandich, Plasma Sources Sci. Technol. **3**, 373 (1994).
[24]G. Selwyn, J. Singh, and R. Bennet, J. Vac. Sci. Technol. A **7**, 2758 (1989).
[25]S. Geha, R. Carlile, J. O'Hanlon, and G. Selwyn, J. Appl. Phys. **72**, 374 (1992).
[26]M. Garrity, T. Peterson, and J. O'Hanlon, J. Vac. Sci. Technol. A **14**, 550 (1996).
[27]G. M. W. Kroesen, W. W. Stoffels, E. Stoffels, M. Haverlag, J. H. W. G. den Boer, and F. J. de Hoog, Plasma Sources Sci. Technol. **3**, 246 (1994).
[28]R. Buss and S. Babu, J. Vac. Sci. Technol. A **14**, 577 (1996).
[29]H. Hahn and R. Averback, J. Appl. Phys. **67**, 1113 (1990).
[30]G. M. Chow, R. L. Holtz, A. Pattnaik, A. S. Edelstein, T. E. Schlesinger, and R. C. Cammarata, Appl. Phys. Lett. **56**, 1853 (1990).
[31]G. Praburam and J. Goree, J. Vac. Sci. Technol. A **12**, 3137 (1994).
[32]W. Hareland, R. Buss, D. Brown, and S. Collins, IEEE Trans. Plasma Sci. **24**, 103 (1996).
[33]G. Praburam and J. Goree, IEEE Trans. Plasma Sci. **24**, 97 (1996).
[34]D. Samsonov and J. Goree, Phys. Rev. E **59**, 1047 (1999).
[35]F. Huang and M. Kushner, J. Appl. Phys. **81**, 5960 (1997).
[36]J. Thornton, J. Vac. Sci. Technol. A **11**, 666 (1974).
[37]N. Laegreid and G. Wehner, J. Appl. Phys. **32**, 365 (1961).